Journal of
Composites Science

MDPI

Article

Biocomposite Based on Polyhydroxybutyrate and Cellulose Acetate for the Adsorption of Methylene Blue

Ángel Villabona-Ortíz [1], Rodrigo Ortega-Toro [2,*] and Jenyfer Pedroza-Hernández [1]

[1] Process Design, and Biomass Utilization Research Group (IDAB) Research Group, Chemical Engineering Department, Universidad de Cartagena, Avenida del Consulado St. 30, Cartagena de Indias 130015, Colombia; avillabonao@unicartagena.edu.co (Á.V.-O.); jpedrozah@unicartagena.edu.co (J.P.-H.)
[2] Food Packaging and Shelf Life (FP&SL) Research Group, Food Engineering Department, Universidad de Cartagena, Avenida del Consulado St. 30, Cartagena de Indias 130015, Colombia
* Correspondence: rortegap1@unicartagena.edu.co

Abstract: Industrialization and globalization have caused severe environmental problems, such as contaminating water bodies by toxic agents from various industries, generating a significant loss of biodiversity and health risks. Globally, approximately 80% of wastewater is discharged without treatment, worsening the situation. However, in Colombia, initiatives have been taken to improve wastewater management, with ambitious investments and targets to improve treatment infrastructure. Recently, advanced technologies have been developed to treat wastewater, including more efficient and sustainable biological methods, such as using coconut-derived adsorbent biomaterials, rich in useful properties for the adsorption of pollutants in solutions. This research focuses on developing a composite biomaterial using cellulose acetate (CA) extracted from coconut mesocarp and polyhydroxy butyrate (PHB), by the casting method, to treat wastewater. Adsorption tests with the tracer methylene blue (MB) were carried out in the Energy and Environment laboratory of the University of Cartagena. For this, MB solutions were prepared with 5 to 50 ppm concentrations. The analyses showed that the composite biomaterial is thermally stable and has good homogeneity and porosity. At a concentration of 40 ppm and a dosage of 10 mg of adsorbent, the adsorption efficiency was 89%, with an adsorption capacity of 35.98 mg/g. The above indicates that the composite biomaterial is presented as a sustainable, improved, and efficient solution to remove contaminants from wastewater, benefiting the environment and human health.

Keywords: composite biomaterial; cellulose acetate; polyhydroxy butyrate; adsorption; wastewater

check for updates

Citation: Villabona-Ortíz, Á.; Ortega-Toro, R.; Pedroza-Hernández, J. Biocomposite Based on Polyhydroxybutyrate and Cellulose Acetate for the Adsorption of Methylene Blue. *J. Compos. Sci.* **2024**, *8*, 234. https://doi.org/10.3390/jcs8070234

Academic Editors: Ahmed Koubaa, Mohamed Ragoubi and Frédéric Becquart

Received: 11 April 2024
Revised: 3 June 2024
Accepted: 19 June 2024
Published: 24 June 2024

Copyright: © 2024 by the authors. Licensee MDPI, Basel, Switzerland. This article is an open access article distributed under the terms and conditions of the Creative Commons Attribution (CC BY) license (https://creativecommons.org/licenses/by/4.0/).

1. Introduction

Industrialization and globalization have generated environmental problems, such as the contamination of water bodies by contaminants from various industries, including mining, the fertilizer industry, the paper industry, oil refining, textile, and metallurgy [1,2]. These contaminants include heavy metals and dyes, and their massive discharge of around 300–500 megatons of wastewater has led to a 30% loss of global biodiversity and risks to human health, such as cancer, organs, and nervous system damage, and even death [3,4].

Globally, approximately 80% of wastewater is discharged directly into the environment without prior treatment, according to a UNESCO report in 2023 [5]. In recent years, advanced technologies have been developed for wastewater treatment, such as physical, chemical and biological methods, achieving significant advances towards more efficient and sustainable techniques [6,7]. These technologies include electrocoagulation, flocculation, reverse osmosis, coagulation and filtration [8,9]. However, these treatment methods have disadvantages, because they can produce secondary contaminants and require a high operating cost [10,11]. Unlike other technologies for treating contaminated water, adsorption stands out as an efficient process, as it is easy to operate, economical, abundant in raw materials, and easy to recover [8,12], with activated carbon and zeolite being the materials

most used in the removal of contaminants by adsorption due to their superior adsorbent characteristics compared to other materials, but it is essential to keep in mind that they also have a higher economic value [13–15]. Studies have been performed to develop more economical and sustainable adsorbent materials to overcome these challenges, made from biological agents such as algae, fungi, bacteria and multiple agro-industrial wastes [16].

Consequently, composite biomaterials have emerged as a viable alternative by combining a polymer matrix with natural fibers, resulting in materials with improved morphological, mechanical, and thermal properties [17]. These composite biomaterials contain lignocellulose, which enhances the adsorption process due to the presence of different functional groups [18].

Coconut, a tropical species that produces fruits in large quantities in Colombia, offers interesting potential as a source of adsorbent biomaterials. Coconut mesocarp (CCM), composed mainly of cellulose, has been studied for its capacity to adsorb contaminants in aqueous solutions [19,20]. In addition, research has been carried out to improve CCM's morphological and physical–chemical properties, as lignocellulosic materials are highly hydrophilic and can present hydrodynamic problems in adsorption systems [21]. For example, Pang et al. [22] prepared a compound for the degradation of methyl orange based on a coconut shell, with several types of metallic and metal-free semiconductors to improve its physical–chemical and optical properties, and the results obtained showed that, by incorporating semiconductors, the biomaterials exhibited better thermal stability, with an increased specific surface area and pore volume. Likewise, Yuan et al. [23] synthesized an adsorbent based on a coconut shell doped with Mg-Al to improve the phosphorus adsorption capacity in wastewater; the results showed an acceptable performance of the adsorbent, with a maximum removal capacity towards phosphorus of 60.39 mg/g at pH 6. Therefore, the importance of developing efficient and sustainable wastewater treatment technologies becomes evident with the growing concern for environmental conservation and public health. However, despite advances in this field, more scientific literature regarding specific biomaterials for removing contaminants in wastewater still needs to be published. Therefore, this study aims to address this gap by developing a composite biomaterial from cellulose acetate (CA) extracted from CCM and polyhydroxy butyrate (PHB) (CA/PHB), with the primary objective being to present the preparation and characterization of the composite biomaterial and evaluate its adsorption capacity using the Methylene Blue (MB) tracer, based on the hypothesis that this composite biomaterial will exhibit high efficiency in the removal of contaminants present in wastewater, due to its improved adsorbent properties. This proposal is innovative, as it introduces a biomaterial based on coconut fiber and PHB for the removal of the MB dye, thus providing relevant information in an area of the scientific literature that lacks significant studies on this approach. The tests were carried out in the Energy and Environment laboratory of the Chemical Engineering Programme of the University of Cartagena, Piedra de Bolívar campus.

2. Materials and Methods

Various reagents, solvents, and laboratory equipment were used in the study. Scharlau brand sodium hydroxide was used to extract the cellulose and adjust the pH. Assuring brand sodium chlorite was used as a bleaching agent in cellulose extraction. PanReac AppliChem acetic acid was used in cellulose bleaching and CA synthesis. Acetic anhydride from SIGMA-ALDRICH was used in CA synthesis. Sulphuric acid from EMSURE was used as a catalyst in the synthesis of CA. As a CA modifier, PHB $(C_4H_6O_2)n$ was imported from Helian Polymers B.V. Its chemical composition includes repeating units of hydroxybutyrate. Furthermore, other solvents and equipment, such as chloroform, acetone, dichloromethane, ethanol, phenolphthalein, a heating plate, an analytical balance, an oven, a UV-VIS spectrophotometer, an electric sieve, a pH meter, ultrasonic equipment, and an orbital shaker, were used.

2.1. Synthesis of Composite Biomaterials

The method used for the synthesis of the composite biomaterials was casting. This method involved dissolving the CA in an acetone solution with a weight ratio of 1:10 for 2 h. On the other hand, PHB was dissolved in 50 mL of dichloromethane at 60 °C under sound energy in ultrasonic equipment for 40 min. Then, 5 mL of the PHB solution was mixed with 20 mL of the acetate solution in a Petri dish. The mixture was kept at room temperature for 24 h to allow the solvents to evaporate [24,25].

2.2. Characterization of Composite Biomaterials

The water absorption test was performed according to ASTM D570-98 [26]. Samples of each material were immersed in water for different periods, recording the weight change at 24-h intervals. For the test, 0.6 g of each material was added to 5 mL of water, following the methodology proposed by Behera et al. [27]. The percentage of water absorption was calculated using Equation (1):

$$\frac{W_F - W_i}{W_i} \times 100 \quad (1)$$

W_F is the sample's weight after absorption, and W_i is the initial weight of the dry sample.

In addition, detailed characterization tests were carried out for the PHB-modified and unmodified (target) biomaterial. The surface charges of the biocomposite were studied using pHpzc, and a thermogravimetric analysis (TGA) was carried out in a Thermogravimetric analyzer, TA INSTRUMENT, Series: 0600-11099, Model: SDTQ600, to determine the composite biomaterials' thermal stability and composition. Fourier transform spectroscopy (FTIR) was used to determine the functional groups in the biomasses and biomaterial composites. This assay was carried out on an IRAffinity-1, FTIRSHI-MADZU, Serie A213749. The samples were prepared before and after adsorption in the best conditions. In a TESCAN, model MIRA 3, scanning electron microscopy (SEM) was carried out to observe the morphological properties of the biomass surface before and after the modifications, while X-ray diffraction (XRD) was carried out on a Malvern-PANalytical Empyrean 2012 model with a Pixel 3D detector, to determine the degree of crystallinity of the biomass before and after the modifications. No special sample preparation was required for these tests.

2.3. Adsorption Tests

A Zero Loading Point test was performed on the prepared materials using sodium hydroxide (NaOH) and 0.1 M hydrochloric acid (HCl) to adjust the pH of the distilled water to a range of 3 to 11. A total of 50 mg of the materials were added to 10 mL centrifuge tubes with 5 mL of distilled water at different pH values and shaken for 24 h. The final pH was measured in each tube and was compared with the initial pH using a graphical method [28].

Solutions with concentrations ranging from 5 to 50 ppm were prepared and analyzed by UV-VIS spectrophotometry at 664 nm to construct the MB calibration curve, establishing a relationship between absorbance and concentration [29].

A one-factor experimental design was performed to evaluate the influence of pH on adsorption capacity. Three pH levels above the zero-loading point (pHpzc) were selected, keeping the initial concentration (40 ppm) and the adsorbent dose (35 mg) constant. A total of 10 mL of MB solution was added to each test tube, and the test tube was left in contact for 24 h. Replicates of the experiment were carried out [30].

The MB mixture with each biomaterial was prepared at initial concentrations ranging from 5 to 100 ppm, with adsorbent doses of 10 to 30 mg, and the pH was adjusted as required. The contact time was 24 h at room temperature, with a solution volume of 10 mL. At the end of the experiment, the concentration was determined by absorbance using the

ratio obtained from the calibration curve. With the data obtained above, the adsorption capacity of MB by samples of the natural biocomposite was determined using Equation (2):

$$Q_T = \frac{(C_o - C_T) \times V}{W} \quad (2)$$

where Q_T (mg/g) is the adsorption amount at equilibrium, C_o (mg/L) is the initial concentration in the liquid phase of the dye, C_T (mg/L) is the concentration at a specific time in the liquid phase of the dye, V (L) is the volume of adsorbate solution and W (g) is the mass of adsorbent used [31].

3. Results

3.1. Preparation of Composite Biomaterials

Cellulose: Two batches of 25 g of precursor were made to carry out the double alkaline extraction and sodium chlorite bleaching methodology. The objective was to determine the average weight loss due to removing lignin, hemicellulose, and other surface compounds in the fiber.

Figure 1 shows the cellulose preparation process, where it is observed that the alkaline extraction solution initially has a brown color due to the presence of traces of lignin and impurities in the fiber. However, the alkaline treatment removes these compounds, as evidenced by the resulting cellulose solution with a yellow color. Through the bleaching process, the lignin is removed by oxidation, resulting in water-soluble compounds and a pure white color. The results obtained from the two precursor batches were 18 g and 20 g of cellulose, respectively, with an efficiency between 72% and 80%. These results are consistent with those reported in other studies, such as the cellulosic fraction obtained from *Thepesia populnea* and areca palm leaf, with efficiencies of 76% and 82%, respectively [32,33]; in this area, researchers have found that the presence of higher cellulose content leads to significant improvements in mechanical properties, such as tensile strength and modulus of elasticity [24].

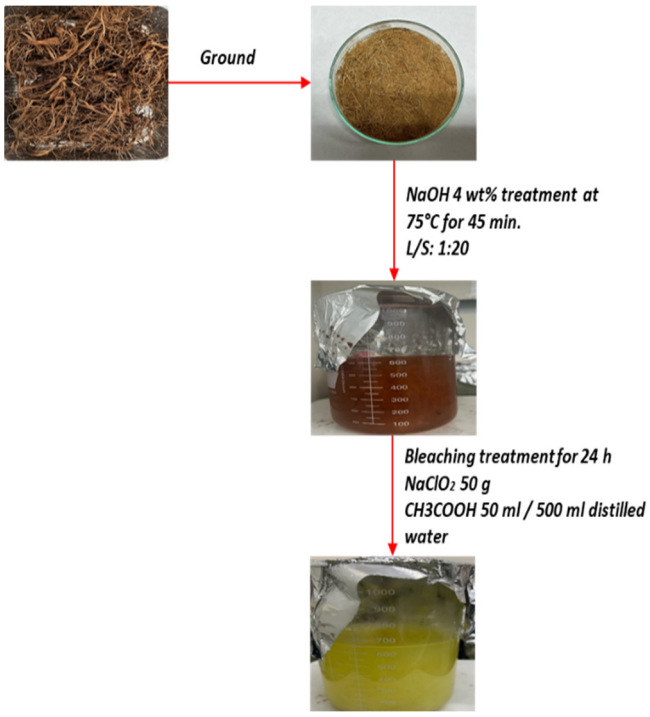

Figure 1. Cellulose extraction and bleaching process.

The purity of the cellulose extracted from the CCM was analyzed by thermogravimetry in a temperature range from 0 °C to 950 °C with a heating rate of 10 °C/min. As a result, it was observed that coconut cellulose has a higher purity compared to commercial cellulose.

3.2. Thermogravimetric Analysis

Figure 2 presents the thermogravimetric analysis for cellulose (Figure 2a) and CA/PHB (Figure 2b); it can be noted that the thermal stability of coconut cellulose is reached at 130 °C, where a mass loss of 3.214% is observed, corresponding to the evaporation of the water present in the biomass. This result suggests that the moisture present in coconut cellulose is lower compared to commercial cellulose, which presents a mass loss between 80 °C and 140 °C [34]. On the other hand, the thermogravimetric analysis of the CA/PHB composite biomaterial was performed between 30 °C and 950 °C at 10 °C/min. Figure 2b shows the results obtained, which present three degradation phases. The first one starts at 100 °C and corresponds to the evaporated water content, equivalent to 0.5%. The second phase corresponds to the degradation of PHB, between 250 °C and 310 °C, with a mass loss of 50%. On the other hand, the last to degrade was CA, from 360 °C with a mass loss of 49.5%. This smaller number of stages and rapid degradation indicates a good adhesion between the lignocellulosic derivative and the polymeric matrix. Moreover, the presence of cellulose esters generates a double peak of mass loss: the first corresponds to the degradation of the acetate, and the second corresponds to the carbonization of the degraded products at elevated temperatures [35].

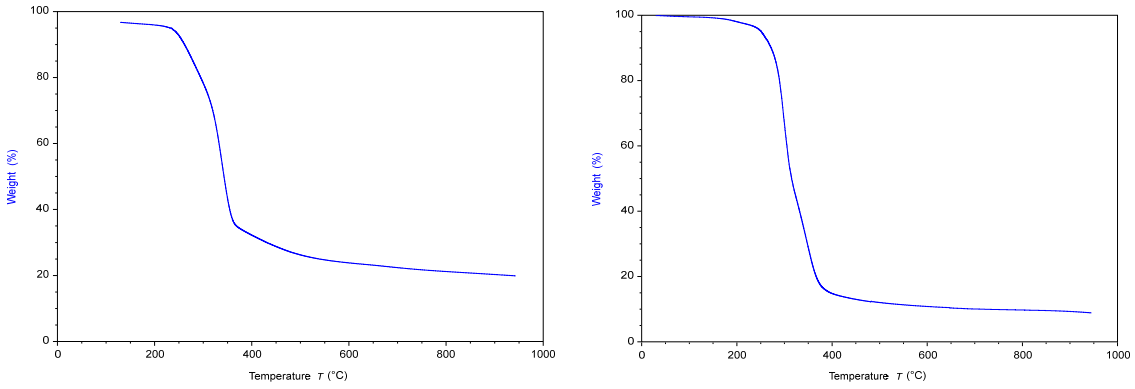

(a) (b)

Figure 2. Thermogravimetric analysis. (**a**) cellulose extracted from CCM. (**b**) CA/PHB.

The mass degradation of coconut cellulose occurs in three stages. The first stage occurs between 250 °C and 350 °C, where a loss of 49.4%, corresponding to hemicellulose, lignin, extractives, and the components present in smaller proportions in the lignocellulosic derivatives, occurs, similar to that reported by Vijay et al. [36]. The second stage of mass degradation occurs between 350 °C and 950 °C, corresponding to cellulose degradation, where a 23.8% mass loss is observed. This result is in agreement with those reported by Satha et al. [34] and Vijay et al. [36], who indicated that cellulose degradation starts at 340 °C and 350 °C, respectively, with mass losses of 11.56% and 12%.

Compared to commercial cellulose, the degradation of coconut cellulose occurs more slowly, indicating the higher thermal stability of the biomass derivative [34].

On the other hand, 5 g of cellulose was used in the acetylation reaction. The experiment was repeated five times without variations in the methodology parameters, such as temperature, time, and number of reagents, to ensure an adequate solid–liquid ratio; as a result, a CA sample was obtained. The reaction yield was evaluated for each set-up, showing an average yield of 89.2 ± 3.65%.

These results are similar to those reported by Guerrero [37] in a study where CA was synthesized from grass, obtaining an average yield of 92.08%. In the present study, a

vacuum membrane filtration method was used to ensure a higher retention of fine particles and tightness, which may have influenced the results obtained [38].

Finally, a composite biomaterial of CA and PHB (CA/PHB) was developed using the casting method. The proportion of PHB in the preparation was based on previous research, showing that higher CA content improves the mechanical and morphological properties of the films [24]. In the preparation of the composite biomaterials, the ratio obtained was taken into account, and the research findings of Abu Aldam et al. were considered [39].

According to Abu Aldam et al. [24], the calculated amount of PHB must be added to 50 mL of dichloromethane. Upon preparation, it was observed that as the amount of CA increases, the composite biomaterial's mass and thickness also increase. For example, the sample with 10 g of CA has a mass of 2.5 g and a thickness of 900 µm. In comparison, the sample with 1 g of CA has a mass of 0.24 g and a thickness of 85 µm, resulting in the different properties and characteristics of the composite biomaterial [24].

3.3. Characterization of the Biomaterial

The water absorption test is one of the most important tests in the analysis of the target composite biomaterial, taking into account that the main property to be modified is the hydrophilic character of the lignocellulosic derivative, which tends to absorb humidity from the air and through direct contact with the source [39]. The purpose of this modification is to avoid caking when scaling up the process in adsorption columns. Therefore, by water adsorption, the efficiency of the polymeric matrix in achieving this objective is determined.

Figure 3 shows the results obtained for the water absorption of the targets and the composite biomaterial. It can be observed that the targets, corresponding to the CCM and cellulose, show a higher absorption than the composite biomaterial in the time evaluated (CA/PHB), reaching a value close to 100%. This is due to the polymeric matrix's hydrophobic nature, which decreases their hydrophilic character. Similarly, Behera et al. [27] performed PHB and PLA coatings on hemp fibers, and observed greater water absorption resistance with coated fibers than uncoated fibers.

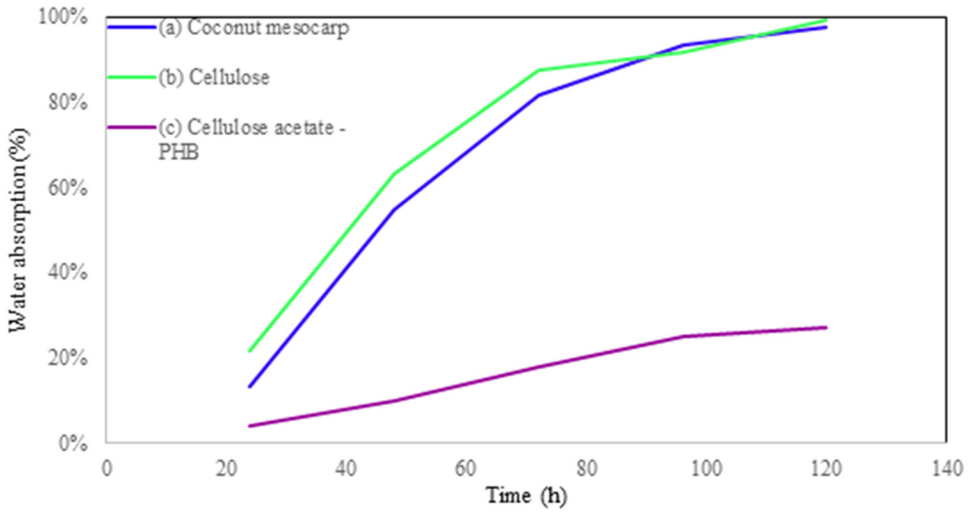

Figure 3. Water absorption study.

In terms of specific results, cellulose showed faster water absorption, reaching 99% at 120 h, while coconut fiber reached 97%. The CA/PHB composite biomaterial reached 27%, respectively. These values remained constant after 120 h.

Based on the results obtained, it was determined that CA/PHB stood out as the biomaterial and the target with the highest water resistance. This phenomenon is due to the chemical modification known as acetylation, which involves substituting the hydroxyl groups in the cellulose chains by acetyl groups. This chemical transformation leads to a significant decrease in the hydrophilic character of the cellulose [40]. Consequently, it is

observed that pure cellulose showed a higher water absorption rate compared to CCM and the CA/PHB composite biomaterial.

These results are consistent with a study by Cindradewi et al. [41], who examined a composite biomaterial based on CA and nano fibrillated cellulose in different proportions and conducted a comprehensive water absorption analysis. Their findings supported the direct relationship between higher cellulose content and water absorption capacity.

3.4. SEM Analysis

Figure 4a,b reveal that the CCM and cellulose exhibit a fibrous and porous morphology. As pointed out by Behera et al., this is a good indicator [27], who claim that the presence of pores indicates a lower tensile strength, implying deficiencies in mechanical properties and limitations in scaling up to adsorption columns.

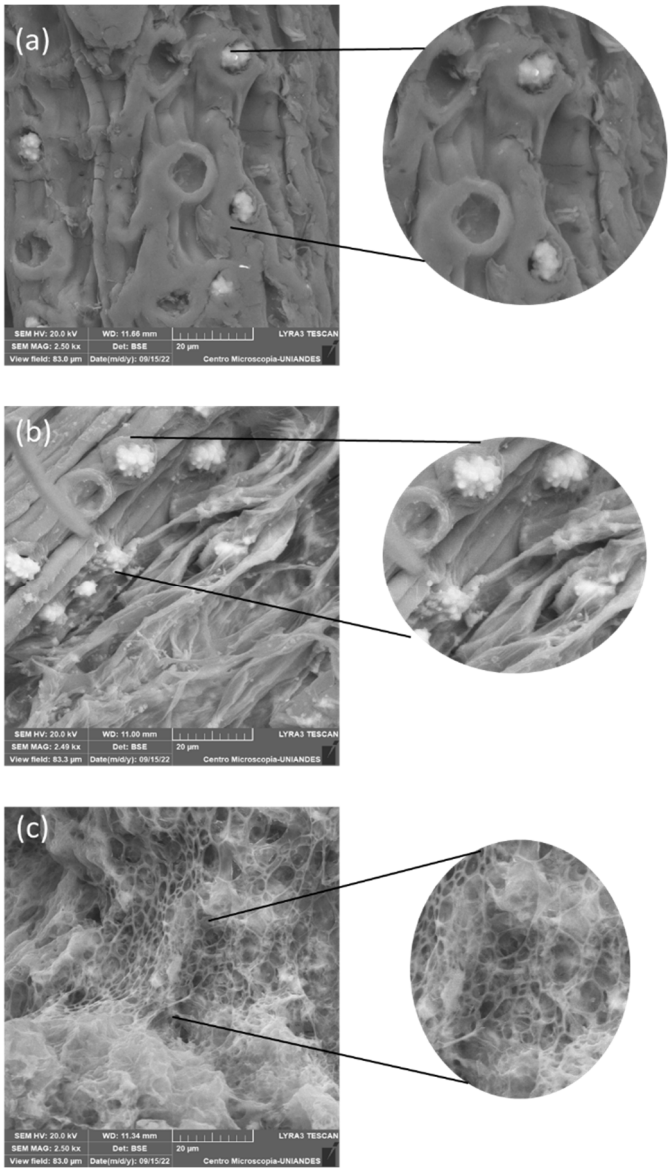

Figure 4. SEM analysis of the materials. (**a**) CCM. (**b**) Cellulose. (**c**) CA/PHB.

The composite biomaterial observed in Figure 4c shows that the CA/PHB film shows a more effective homogenization of the components. In addition, it is observed that the biopolymer layers are thin. This inhomogeneous distribution and the thinness of the biopolymer layers may be related to a higher water resistance in the presence of PHB [27].

These findings are especially notable in the case of CA, where its porous structure is significantly improved after modification with PHB.

By showing a porous structure in the PHB, this composite biomaterial presents advantages for adsorption, as the pores provide available sites for the penetration of contaminant molecules into the functional groups present in the lignocellulosic derivatives. These findings are consistent with Zhu et al.'s previous research [42].

The modification of cellulose acetate is a process to improve the mechanical properties of the biomaterial, as demonstrated in Figure 4. The analysis reveals the formation of a thin film of biopolymer on the surface of the cellulose acetate, which plays a fundamental role in giving it hydrophobic characteristics. Originally, cellulose biomass was very hydrophilic, which limits its efficiency in adsorption applications in aqueous solutions. However, by converting it into cellulose acetate, a significant transformation is achieved, improving its mechanical properties for the adsorption of the contaminant under study. This modification not only improves the mechanical characteristics of the biomaterial but also optimizes its hydraulic properties, since the thin film that adheres to the material prevents the formation of agglomerations during the adsorption process. This fact means that, from a physical point of view, the efficiency and effectiveness of the adsorption process, and the hydraulic properties, are also improved.

3.5. XRD Analysis for the CA/PHB

CA/PHB analysis was performed to evaluate the organization of the chains and molecular interactions in the material (Figure 5).

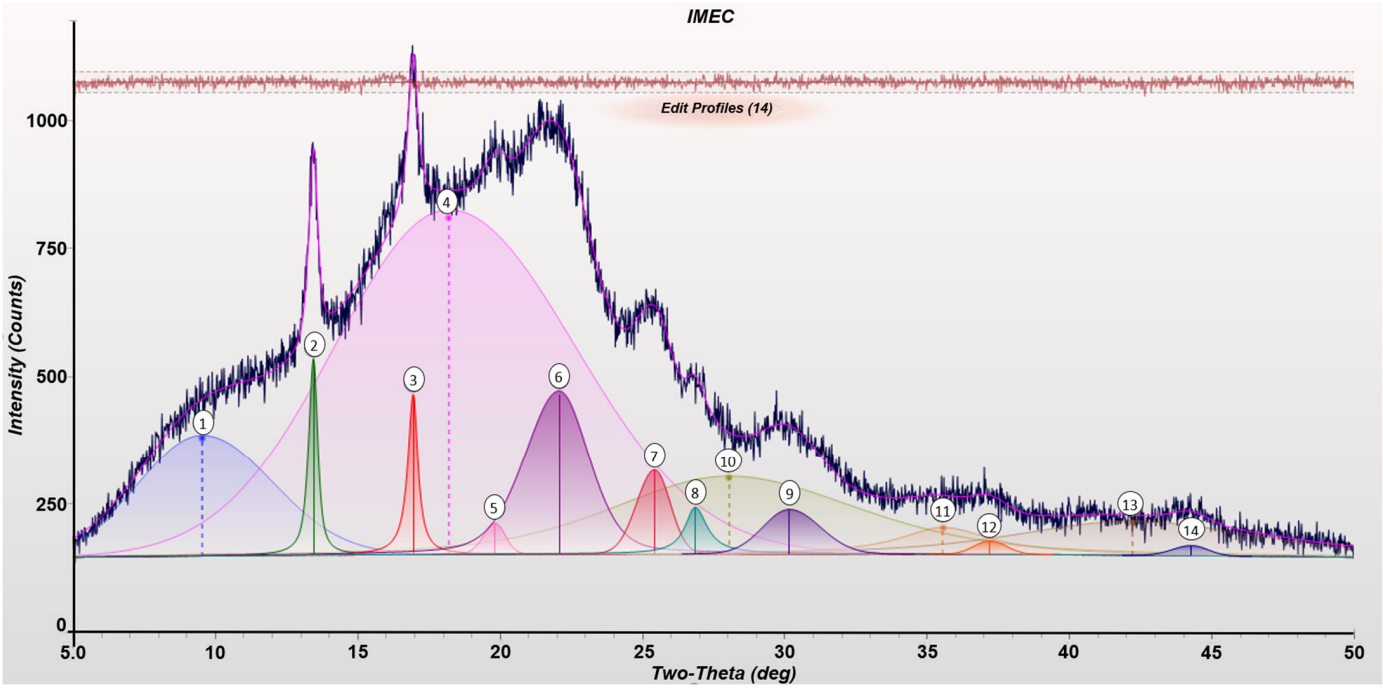

Figure 5. XRD analysis of CA/PHB.

The figure above shows that the CA/PHB composite biomaterial has an amorphous structure. The crystallinity determined was 2.09% for CA/PHB. These results are attributed to the fact that the acetyl groups occupy less space than the hydroxyl (OH) groups, which reduces the molecular interactions and, thus, the crystallinity of the material [27]. Despite this, a slight increase in the crystallinity of CA/PHB is observed. This increase is due to PHB, which tends to induce a crystalline structure during polymerization [27].

3.6. FTIR Analysis before Adsorption

FTIR analysis was performed on all materials before adsorption to determine the surface functional groups present, which are responsible for the bonds between adsorbates and adsorbents [43].

Figure 6 shows the FTIR graphs of the materials with similar structures before adsorption. In all figures, there was a peak in the area of single bonds (2500–4000 cm^{-1}) in the range of 3200–3500 cm^{-1}, indicating the presence of hydrogen bonds and the vibration of OH-, COOH, and NHx functional groups, as in cellulose and hemicellulose [30].

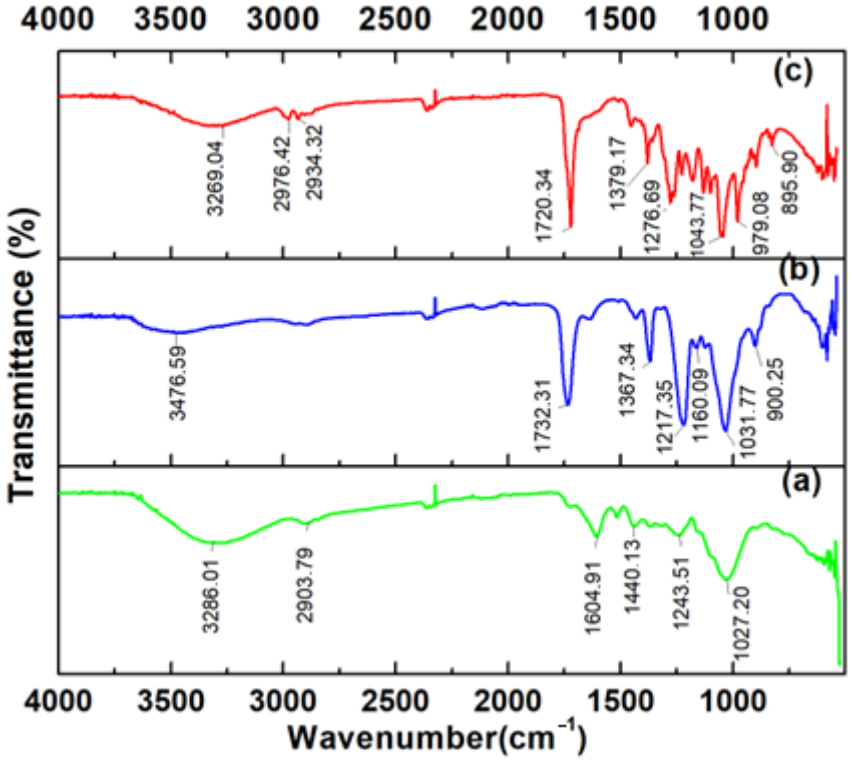

Figure 6. FTIR analysis before adsorption tests. (**a**) CCM. (**b**) Cellulose. (**c**) CA/PHB.

The peaks 2860 cm^{-1} and 2935 cm^{-1} correspond to aliphatic compounds or their derivatives, such as methylene [44]. In the double bond range (1500 cm^{-1} to 2000 cm^{-1}), a characteristic band can be observed between 1650 cm^{-1} and 1850 cm^{-1} in all spectra, suggesting the presence of carbonyl groups and aromatic rings associated with lignin [45]. Peaks between 1490 cm^{-1} and 829 cm^{-1} correspond to the CH, OH, and C-O bonds present in cellulose [46]. Within the 400 cm^{-1} to 600 cm^{-1}, peaks with medium to high intensity of aromatic groups are detected, representing double bonds.

For cellulose (Figure 6c), a characteristic peak is observed at 3476.59 cm^{-1}, indicating that it contains free -OH groups, which is consistent with the expected chemical composition of cellulose [47].

The CA/PHB composite biomaterial shows a peak at 1720 cm^{-1} due to the carbonyl groups present in the biopolymer, confirming that a homogeneous mixture of both materials was obtained.

3.7. Adsorption Test

3.7.1. Influence of pH on the Adsorption Test

The pHpzc is the pH at which the number of negative charges is equal to the number of positive charges on the surface of a solid material. If the pH is lower than the pHpzc, the solid is positively charged; if the pH is higher than the pHpzc, it is negatively charged. This property indicates the pH range in which the material has an affinity to adsorb ions,

either anions or cations [48]. To determine the pHpzc, the initial pH and the ΔpH were recorded after a contact time between the materials and distilled water at an adjusted pH.

It can be observed that the ΔpH values are higher in general in the presence of PHB, comparing the results obtained from the different materials, indicating a more significant influence on the pH change. To determine pHpzc, initial pH vs. ΔpH was graphed (Figure 7) and identified by cutting the abscissa on the curve for each material.

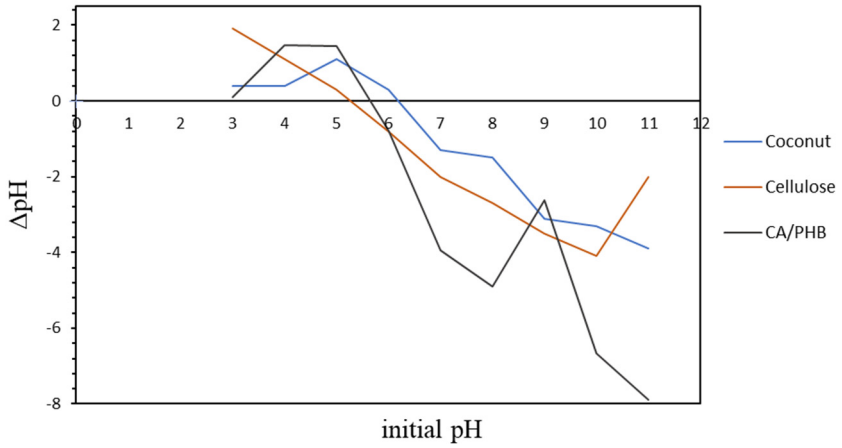

Figure 7. Analysis of the pH zero point of materials.

There are no references in the literature regarding the pHpzc of the prepared composite biomaterials and PHB; however, such information has been evaluated for other composites, which agree that the target and the CA/PHB composite biomaterial have the same pHpzc value or are close, as determined by Shoukat et al. [49], who prepared a mango seed composite biomaterial and obtained a pHpzc of 6.5 for the target and 6.4 for the biocomposite.

According to the results obtained, and considering that MB is a cationic dye, adsorption tests were performed using a pH higher than the pHpzc of each adsorbent to favor the adsorption of these species. A calibration curve was constructed using linear regression to predict concentrations based on the spectrophotometer's response to known standards. The absorbance was recorded at a wavelength of 664 nm [50]. For this purpose, MB solutions with concentrations of 5, 10, 15, 20, 25, 25, 30, 35, 40, 45 and 50 ppm were prepared (Figure 8).

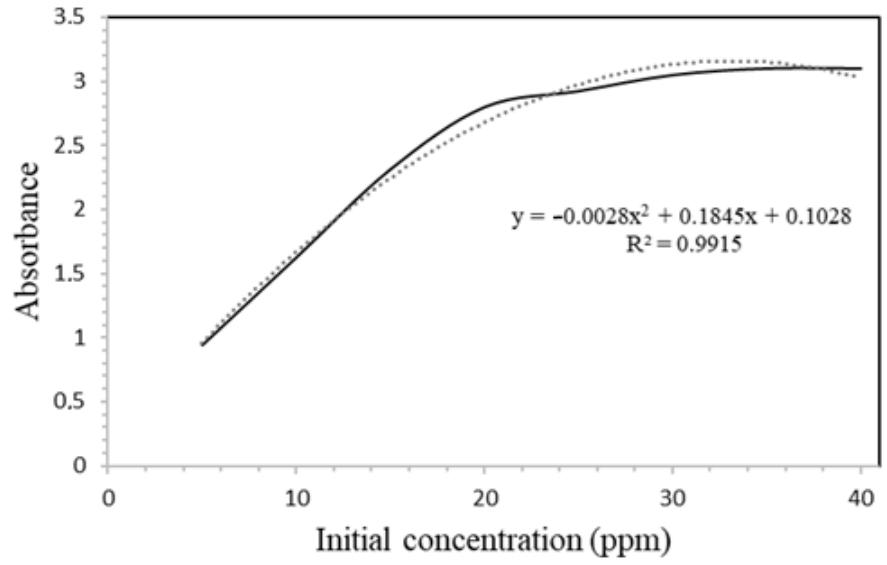

Figure 8. Calibration curve of methylene blue.

As can be seen in Figure 8, the mathematical model that best fits the data is quadratic with 0.9915. From the quadratic model, the variable x was solved to obtain an equation of concentration (x) as a function of absorbance (y):

$$Co = -0.1845 \pm \frac{\sqrt{0.03515 - 0.0112(A)}}{-0.0056} \quad (3)$$

The initial pH of the solutions is a crucial factor in the adsorption capacity because it affects the ionization of the adsorbate, the dissociation of the functional groups on the active sites of the adsorbent, and its surface charge. When the pH of the solution is higher than pHpzc, the electrostatic forces increase, especially when the dye molecules are negatively charged and the adsorbent surface [51,52].

Figure 9 shows that CCM (a) has the highest adsorption efficiency under the same adsorbent dose and initial concentration conditions. On the other hand, the bio-material CA/PHB (c) shows the lowest efficiency, as observed in the figure. The above is because coconut mainly contains lignin, giving it an advantage over cellulose. Cellulose, having OH groups, has a degree of alkalinity that does not contribute to the electrostatic attraction between the adsorbent and the adsorbate, taking into account that MB is cationic [53].

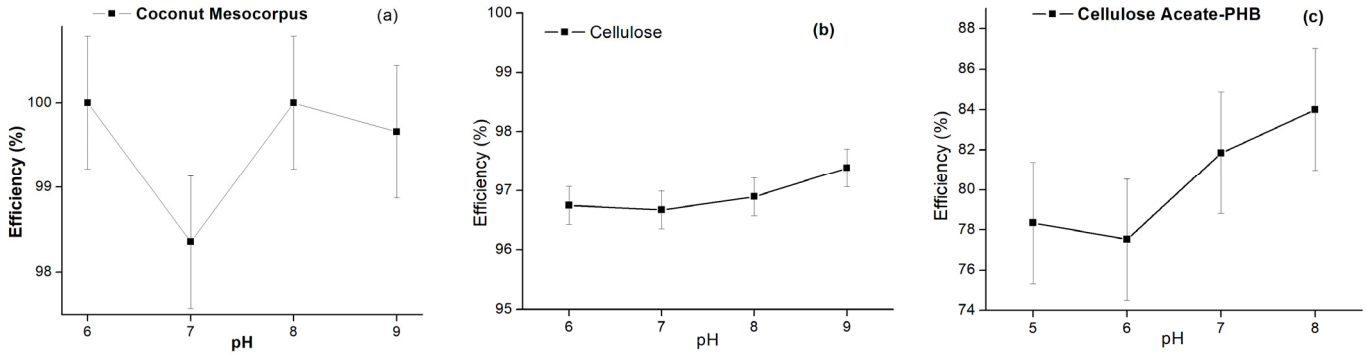

Figure 9. Effect of pH on adsorption efficiency capacity. (**a**) CCM. (**b**) Cellulose and (**c**) CA/PHB dosage.

The CCM showed a high adsorption efficiency at pH 6 and pH 8, reaching 100% efficiency with an adsorption capacity of 11.43 mg/g and a deviation index of 0–0.05 for each pH, confirming the reliability of the results [51]. Studies by other researchers support these findings, such as the one by Etim et al. [54], who obtained the highest adsorption efficiency at pH 6, with 99.2%, using coconut fiber. In addition, de Oliveira et al. [55] determined that the adsorption equilibrium is reached at pH 7, as the efficiency remains constant above this value.

Cellulose (Figure 9b) showed a high adsorption efficiency at pH 8, reaching 97.38% efficiency and an adsorption capacity of 11.01 mg/g, with a deviation rate between 0.06–1.3 for each pH. These results are consistent with a previous study by Benhalima and Ferfera-Harrar [56], who found that carboxymethyl cellulose and dextran sulphate films achieved an adsorption efficiency of 98% for MB at pH 8.

It was observed that the CA/PHB biomaterial composite showed a higher adsorption efficiency at pH 8, with 84%, and an adsorption capacity of 9.59 mg/g. These results are consistent with a previous study by Wang et al. [57], which showed an increase in adsorption efficiency over a pH range of 6 to 9, followed by a decrease above 9.

In general, the results obtained confirm the expected behavior: an increase in pH increases the adsorption efficiency of MB. The above is due to the deprotonation of the active sites of the adsorbent, which favors the electrostatic attraction between the dye positively charged and the adsorbent negatively charged. However, in cases where efficiency decreases with increasing pH, it is attributed to hydrolysis of the adsorbent, which generates positively charged active sites [52,58].

3.7.2. Effect of Adsorbent Dosage on Adsorption Efficiency

The adsorption capacity depends on several factors, including the pH of the solution, contact time, temperature, adsorbent dosage, and initial concentration [59]. For this study, the variables analyzed were the dose of the prepared materials and the initial concentration of MB. Figure 10 shows the results obtained from the experimentation.

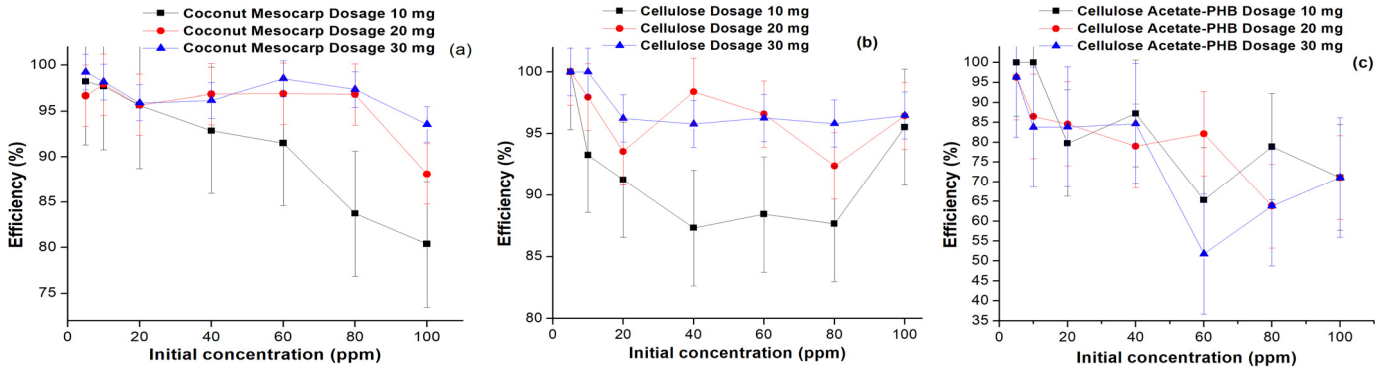

Figure 10. Analysis of the effect of adsorbent dosage on adsorption efficiency. (**a**) CCM. (**b**) Cellulose and (**c**) CA/PHB.

The adsorption capacity is closely related to the adsorbent dose, as it determines the degree of adsorption and the amount of material required per solution unit. With increasing adsorbent dosage, keeping all other parameters constant, the adsorption efficiency initially increases, reaches a maximum, and then decreases due to the saturation of the active sites of the adsorbent [60].

Figure 10a shows that at an initial concentration of 5 ppm and adsorbent doses of 10, 20, and 30 mg, the adsorption efficiency of the CCM remains constant at a maximum of 100%. The above is due to the low concentration of the contaminant, which facilitates mass transfer and increases the adsorption efficiency, regardless of the adsorbent dose [52,59]. However, at a concentration of 40 ppm, the adsorbent dosage follows a gradually increasing pattern, reaching a maximum and then decreasing due to possible aggregation of adsorbent particles, reducing the effective surface area [61]. In the case of cellulose, high adsorption efficiencies are observed in Figure 10b, with a range of 85–100%. It is shown that increasing the adsorbent dose increases the adsorption efficiency, except at a concentration of 40 ppm, where the maximum is reached at 20 mg (98% efficiency) and then decreases to 30 mg (96% efficiency) [62].

In Figure 10c, the CA/PHB composite biomaterial showed a behavior attributed to its acidic surface and the early saturation of the adsorbent for the assigned solution volume and concentration [63], but with a decrease in adsorption efficiency due to the crystallinity of PHB. At a concentration of 20 ppm, a maximum expected efficiency of 88.15% was reached with an adsorbent dose of 20 mg.

The results of the adsorption experiments showed that, at an initial concentration of 5 ppm, the highest adsorption efficiency values were obtained (between 98% and 99%). However, as the initial concentration increased (from 80 ppm), a gradual decrease in the adsorption percentage was observed, reaching its lowest point at 100 ppm (80%). These results are consistent with previous findings indicating that, at low initial concentrations, sufficient active sites are available for adsorption. Still, as the concentration increases, the availability of active sites decreases [64]. Furthermore, the adsorption capacity of the CCM was found to increase at higher concentrations due to the saturation of the material. These findings emphasize the importance of considering the initial concentration in the adsorption process and its impact on the efficiency and adsorption capacity of the adsorbent.

Adsorption tests were conducted to investigate the effect of increasing the initial MB concentration on cellulose purified from CCM. High adsorption percentages (between 99% and 99.5%) were obtained at low concentrations, indicating that cellulose-rich lignocellu-

losic materials exhibit good adsorption behavior. As the initial concentration increased, the adsorption efficiency decreased, but it was observed that the minimum value did not drop below 87% for a small adsorbent dose; this suggests that the material has a larger number of chemical species involved in the adsorption process. Furthermore, in agreement with the reports of Alibak et al. [65], it was observed that as the initial concentration increased, the adsorption capacity of the material increased due to the higher amount of chemical species present in the MB deposited on the cellulose surface.

The adsorption capacity of the CA/PHB biomaterial is significantly affected by increasing the initial concentration, resulting in a decreased adsorption efficiency. These results can be explained by the reduction in the availability of active adsorption sites due to the adsorbent surface's modified mechanical and morphological properties as a consequence of PHB [60]. An efficiency range between 50% and 100% was observed, with the lowest concentrations reaching the highest efficiency values. Overall, the composite biomaterial showed a lower performance as an adsorbent compared to the target materials.

3.7.3. FITR Analysis after Adsorption Process

Figure 11 presents the FTIR spectra of all materials after adsorption. Decreases in the intensity of the peaks are observed compared to the initial spectra. The peak corresponding to the OH- and NHx vibration between 3200 cm^{-1} and 3500 cm^{-1} shows a decrease in intensity in all materials [30]. In the regions of 2800 cm^{-1} to 3000 cm^{-1}, a decrease in the peaks corresponding to aliphatic compounds can be observed [45]. The peaks related to the carbonyl groups between 1650 cm^{-1} and 1850 cm^{-1} decrease, except for cellulose and CA/PHB, which show a high intensity [46]. Peaks in 1490 cm^{-1} to 829 cm^{-1}, corresponding to CH, OH, and C-O bonds, decrease in all cases [46]. The decrease or disappearance of the peaks indicates the capture of the dye in the active sites of the adsorbents. In addition, peaks between 800 cm^{-1} and 1000 cm^{-1} correspond to NH chromophores and C-S functional groups in the MB [66].

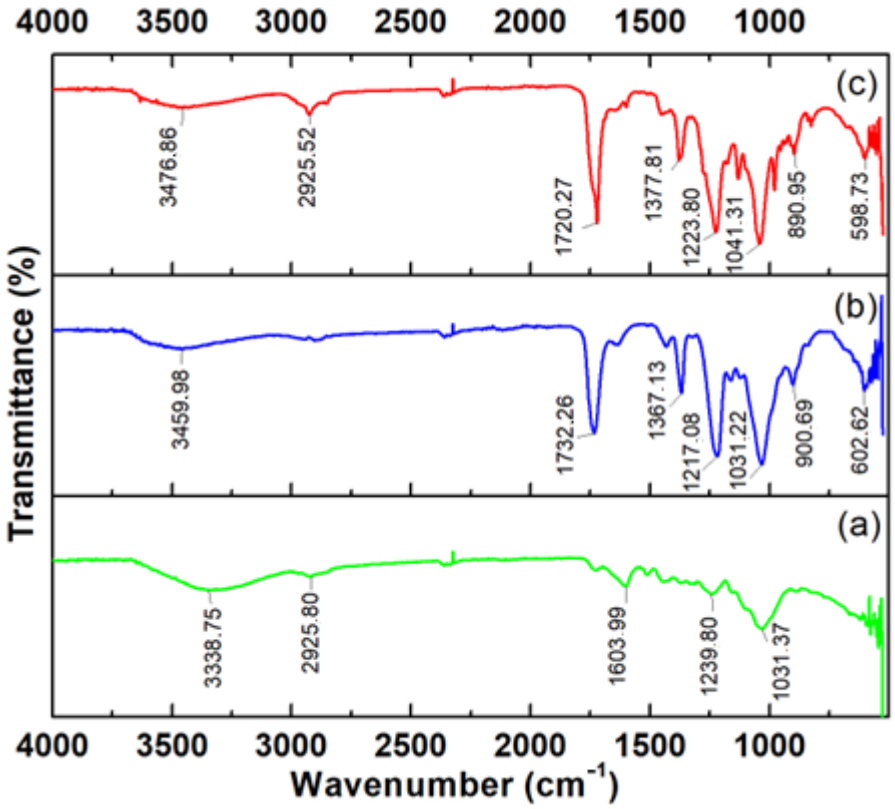

Figure 11. FTIR analysis after adsorption tests. (**a**) CCM. (**b**) Coconut cellulose. (**c**) CA/PHB.

These results indicate that the CA/PHB biomaterial is offered as an adsorbent for application in the treatment of wastewater contaminated with heavy metals or dyes due to its adequate characteristics in terms of its high homogeneity and porosity, water resistance, thermal stability, good adhesion of the polymer matrix to the fiber and high adsorption efficiency, achieving 89% removal of the contaminant, as well as its biological origin and the ability to be produced economically.

For a comprehensive view of the CA/PHB biomaterial's effectiveness and versatility, We present a comparison in Table 1 with other materials commonly used for treating contaminated water. The data clearly show that, in many instances, the CA/PHB biomaterial outperforms its counterparts, often achieving higher removal capacities even with a lower dosage.

Table 1. Comparison with other related studies.

Precursor	Synthesis Variables		Contaminate Removed	Removal Capacity (mg/g)	pH	Adsorbent Dose (g)	Pollutant Concentration (mg/L)	Reference
Mesoporous carbon grafted with aminosilane	T (°C)	60	Tartrazine	143.09 in 2 h	6	0.02	12.5–250	[67]
	t (h)	6						
	Modification	Impregnation with $LaCl_3$						
Raw sawdust	T (°C)	700	Indigo Carmine	9.39 in 3 h	2.5	5	10–50	[68]
	t (h)	2						
	Modification	Activation with NaOH						
Banana peels	T (°C)	60	Zn(II)	25.59 in 2 h	5	1	50	[69]
	t (h)	24						
	Modification	Modified with NaOH and $Ca(CH_3OO)_2$						
Passion fruit peels	T (°C)	60		27.48 in 2 h	5	1	50	
	t (h)	24						
	Modification	Modified with NaOH and $Ca(CH_3OO)_2$						
Orange peels	T (°C)	60		16.61 in 2 h	5		50	
	t (h)	24						
	Modification	Modified with NaOH and $Ca(CH_3OO)_2$						
Coconut shell	T (°C)	100	Methylene blue	50.6 in 1 h	8	0.02–0.2	25–200	[70]
	t (h)	24						
	Modification	Activation with H_2SO_4						
Millettia Thonningii seed pod	T (°C)	400	Methylene blue	2.55 in 3 h	7	0.5	10–50	[71]
	t (h)	0.5						
	Modification	Activation with H_3PO_4 (2:1)						

Table 1. *Cont.*

Precursor	Synthesis Variables		Contaminate Removed	Removal Capacity (mg/g)	pH	Adsorbent Dose (g)	Pollutant Concentration (mg/L)	Reference
Aspidosperma polyneuron sawdust	T (°C)	250	Methylene blue	12.45 in 24 h	7	3.5	60	[9]
	t (h)	0.5						
	Modification	H_3PO_4 urea 6 M						
Coconut shell	T (°C)	60	Methylene blue	35.98 in 24 h	8	0.01	40	Present study
	t (h)	24						
	Modification	Modified with polyhydroxybutyrate (PHB)						

4. Discussion

The results obtained in this study provide a detailed understanding of the influence of pH and the initial concentration on MB adsorption efficiency using different adsorbent materials.

First, each adsorbent's zero charge point (pHpzc) was determined, which is the pH at which the net charge on the material's surface is equal to zero. This parameter is crucial, as it influences the electrostatic interactions between the adsorbate and the adsorbent. The results showed that the CCM had a pHpzc of 6, while the cellulose had a pHpzc of 8. These values indicate that the CCM is positively charged at a pH below 6 and negatively charged at a pH above 6. In contrast, the cellulose is positively charged at a pH below 8 and negatively charged at a pH above 8. These findings are consistent with previous studies investigating the pHpzc of similar materials [49,51].

The results of adsorption tests revealed that both CCM and cellulose showed high adsorption efficiencies at pH 6 and 8, respectively. These results are consistent with previous studies that have demonstrated the higher affinity of these materials for MB in these pH ranges [54,57]. The CA/PHB biomaterial, on the other hand, also shows remarkable adsorption efficiency at pH 6, 7, and 8. These results indicate that the addition of PHB does not significantly affect the adsorption capacity of the composite materials compared to their counterparts. However, a slight decrease in adsorption efficiency at pH 8 was observed for the CA/PHB composite biomaterial. This decrease may be attributed to the crystallinity of PHB, which may affect the availability of active sites on the surface of the adsorbent [63].

Likewise, it was observed that at low concentrations of MB (5 ppm), all adsorbent materials showed high adsorption efficiencies, reaching values close to 100%. As the initial concentration increased, the adsorption efficiency gradually decreased. This behavior can be explained by competition between the dye species for the active sites of the adsorbent. At low concentrations, sufficient active sites are available for adsorption, resulting in high efficiency. However, as the concentration increases, active site availability decreases, reducing adsorption efficiency [64].

Finally, an FTIR analysis was performed after the adsorption tests to investigate the interactions between the adsorbate and the adsorbent. The FTIR spectra showed decreases in the intensity of the peaks corresponding to the functional groups on the MB. These changes indicate the adsorption of the dye on the active sites of the adsorbent materials.

5. Conclusions

Cellulose extraction was successful, with a yield between 72% and 80%, indicating no significant loss of precursor material. The preparation of the composite biomaterial showed good adhesion of the polymeric matrix to the fiber, and the CA/PHB was observed to be thermally stable and composed mainly of PHB.

Scanning electron microscopy (SEM) analysis revealed that the CA/PHB composite biomaterial showed better homogeneity and porosity. In water absorption tests, it was determined that this material showed a higher water resistance. FTIR analysis confirmed the presence of characteristic functional groups in the extracted cellulose, CA, and composite biomaterials. In addition, CA/PHB was observed to be less amorphous in X-ray diffraction (XRD) analysis.

Similarly, the optimal pH for CA/PHB was found to be 8. The CCM showed the best adsorbent performance, but the CA/PHB composite biomaterial also presented a high adsorption efficiency at low initial concentrations. At a concentration of 40 ppm and a dose of 10 mg adsorbent, an efficiency of 89% and an adsorption capacity of 35.98 mg/g was achieved. These results highlight the promising adsorption capacity of the composite biomaterial.

Author Contributions: Conceptualization, J.P.-H., Á.V.-O. and R.O.-T.; methodology, Á.V.-O., R.O.-T. and J.P.-H.; experimental work, J.P.-H., software, R.O.-T.; validation, R.O.-T., formal analysis, R.O.-T., and J.P.-H.; investigation, J.P.-H., R.O.-T. and Á.V.-O.; resources, Á.V.-O.; data curation, R.O.-T. and Á.V.-O.; writing—original draft preparation, R.O.-T. and J.P.-H.; writing—review and editing, R.O.-T. and Á.V.-O.; visualization, R.O.-T.; supervision, Á.V.-O. and R.O.-T.; project administration, Á.V.-O. and R.O.-T.; funding acquisition, Á.V.-O. All authors have read and agreed to the published version of the manuscript.

Funding: This research received no external funding.

Data Availability Statement: The data that support the results of this study are available on request from the corresponding author.

Acknowledgments: The authors thank to the University of Cartagena for providing the materials and equipment required to carry out the study.

Conflicts of Interest: The authors declare no conflicts of interest.

References

1. Chong, Z.T.; Soh, L.S.; Yong, W.F. Valorization of agriculture wastes as biosorbents for adsorption of emerging pollutants: Modification, remediation and industry application. *Results Eng.* **2023**, *17*, 100960. [CrossRef]
2. Ahmadian, M.; Derakhshankhah, H.; Jaymand, M. Recent advances in adsorption of environmental pollutants using metal–organic frameworks-based hydrogels. *Int. J. Biol. Macromol.* **2023**, *231*, 123333. [CrossRef] [PubMed]
3. Ahmad, A.; Kamaruddin, M.A.; Abdul, A.K.; Yahya, E.B.; Muhammad, S.; Rizal, S.; Ahmad, M.I.; Surya, I.; Abdullah, C.K. Recent Advances in Nanocellulose Aerogels for Efficient Heavy Metal and Dye Removal. *Gels* **2023**, *9*, 416. [CrossRef] [PubMed]
4. Sarria, N.V.; Rivera Velasco, D.M.; Larrahondo Chávez, D.A.; Mazuera Ríos, H.D.; Gandini Ayerbe, M.A.; Goyes López, C.E.; Mejía Villareal, I.M. Struvite and hydroxyapatite recovery from wastewater treatment plant at Autónoma de Occidente University, Colombia. *Case Stud. Chem. Environ. Eng.* **2022**, *6*, 100213. [CrossRef]
5. UNESCO The United Nations World Water Development Report 2023: Partnerships and Cooperation for Water. *UNESDOC*. 2023. Available online: https://unesdoc.unesco.org/ark:/48223/pf0000384655 (accessed on 21 March 2024).
6. Saeed, Q.; Xiukang, W.; Haider, F.U.; Kučerik, J.; Mumtaz, M.Z.; Holatko, J.; Naseem, M.; Kintl, A.; Ejaz, M.; Naveed, M.; et al. Rhizosphere Bacteria in Plant Growth Promotion, Biocontrol, and Bioremediation of Contaminated Sites: A Comprehensive Review of Effects and Mechanisms. *Int. J. Mol. Sci.* **2021**, *22*, 10529. [CrossRef] [PubMed]
7. Hsu, C.Y.; Ajaj, Y.; Mahmoud, Z.H.; Kamil Ghadir, G.; Khalid Alani, Z.; Hussein, M.M.; Abed Hussein, S.; Morad Karim, M.; Al-khalidi, A.; Abbas, J.K.; et al. Adsorption of heavy metal ions use chitosan/graphene nanocomposites: A review study. *Results Chem.* **2024**, *7*, 101332. [CrossRef]
8. Bahjat Kareem, A.; Al-Rawi, U.A.; Khalid, U.; Sher, F.; Zafar, F.; Naushad, M.; Nemțanu, M.R.; Lima, E.C. Functionalised graphene oxide dual nanocomposites for treatment of hazardous environmental contaminants. *Sep. Purif. Technol.* **2024**, *342*, 126959. [CrossRef]
9. Ortega-Toro, R.; Villabona-Ortíz, Á.; Tejada-Tovar, C.; Herrera-Barros, A.; Cabrales-Sanjuan, D. Use of Sawdust (*Aspidosperma polyneuron*) in the Preparation of a Biocarbon-Type Adsorbent Material for Its Potential Use in the Elimination of Cationic Contaminants in Wastewater. *Water* **2023**, *15*, 3868. [CrossRef]
10. Díaz, B.; Sommer-Márquez, A.; Ordoñez, P.E.; Bastardo-González, E.; Ricaurte, M.; Navas-Cárdenas, C. Synthesis Methods, Properties, and Modifications of Biochar-Based Materials for Wastewater Treatment: A Review. *Resources* **2024**, *13*, 8. [CrossRef]
11. Younas, F.; Mustafa, A.; Farooqi, Z.U.R.; Wang, X.; Younas, S.; Mohy-Ud-din, W.; Hameed, M.A.; Abrar, M.M.; Maitlo, A.A.; Noreen, S.; et al. Current and Emerging Adsorbent Technologies for Wastewater Treatment: Trends, Limitations, and Environmental Implications. *Water* **2021**, *13*, 215. [CrossRef]

12. Subash, A.; Naebe, M.; Wang, X.; Kandasubramanian, B. Tailoring electrospun nanocomposite fibers of polylactic acid for seamless methylene blue dye adsorption applications. *Environ. Sci. Pollut. Res.* **2024**, *1*, 1–25. [CrossRef] [PubMed]
13. Russo, N.; Sabir, A.; Ortega, D.H.; Quach, Q.; Abdel-Fattah, T.M. Application of Novel Magnetic Activated Carbon-Zeolite Y-Alginate Composites for Removing Organic Dyes. *ECS Meet. Abstr.* **2023**, *65*, 3025. [CrossRef]
14. Ismail, U.M.; Vohra, M.S.; Onaizi, S.A. Adsorptive removal of heavy metals from aqueous solutions: Progress of adsorbents development and their effectiveness. *Environ. Res.* **2024**, *251*, 118562. [CrossRef] [PubMed]
15. Ritter, M.T.; Lobo-Recio, M.Á.; Padilla, I.; Nagel-Hassemer, M.E.; Romero, M.; López-Delgado, A. Adsorption of Safranine-T dye using a waste-based zeolite: Optimization, kinetic and isothermal study. *J. Ind. Eng. Chem.* **2024**, *136*, 177–187. [CrossRef]
16. Mubashar, M.; Naveed, M.; Mustafa, A.; Ashraf, S.; Baig, K.S.; Alamri, S.; Siddiqui, M.H.; Zabochnicka-świątek, M.; Szota, M.; Kalaji, H.M. Experimental Investigation of Chlorella vulgaris and *Enterobacter* sp. MN17 for Decolorization and Removal of Heavy Metals from Textile Wastewater. *Water* **2020**, *12*, 3034. [CrossRef]
17. Zarna, C.; Opedal, M.T.; Echtermeyer, A.T.; Chinga-Carrasco, G. Reinforcement ability of lignocellulosic components in biocomposites and their 3D printed applications—A review. *Compos. Part C Open Access* **2021**, *6*, 100171. [CrossRef]
18. Wang, R.F.; Deng, L.G.; Li, K.; Fan, X.J.; Li, W.; Lu, H.Q. Fabrication and characterization of sugarcane bagasse–calcium carbonate composite for the efficient removal of crystal violet dye from wastewater. *Ceram. Int.* **2020**, *46*, 27484–27492. [CrossRef]
19. Sukmono, Y.; Kristanti, R.A.; Foo, B.V.; Hadibarata, T. Adsorption of Fe and Pb from Aqueous Solution using Coconut Shell Activated Carbon. *Biointerface Res. Appl. Chem.* **2024**, *14*, 30.
20. Chaudhary, S.; Goyal, S.; Umar, A. Fabrication of biogenic carbon-based materials from coconut husk for the eradication of dye. *Chemosphere* **2023**, *340*, 139823. [CrossRef]
21. Benito-González, I.; López-Rubio, A.; Gómez-Mascaraque, L.G.; Martínez-Sanz, M. PLA coating improves the performance of renewable adsorbent pads based on cellulosic aerogels from aquatic waste biomass. *Chem. Eng. J.* **2020**, *390*, 124607. [CrossRef]
22. Pang, Y.L.; Law, Z.X.; Lim, S.; Chan, Y.Y.; Shuit, S.H.; Chong, W.C.; Lai, C.W. Enhanced photocatalytic degradation of methyl orange by coconut shell–derived biochar composites under visible LED light irradiation. *Environ. Sci. Pollut. Res.* **2021**, *28*, 27457–27473. [CrossRef]
23. Yuan, J.; Zhu, Y.; Wang, J.; Gan, L.; He, M.; Zhang, T.; Li, P.; Qiu, F. Preparation and application of Mg–Al composite oxide/coconut shell carbon fiber for effective removal of phosphorus from domestic sewage. *Food Bioprod. Process.* **2021**, *126*, 293–304. [CrossRef]
24. Abu Aldam, S.; Dey, M.; Javaid, S.; Ji, Y.; Gupta, S. On the Synthesis and Characterization of Polylactic Acid, Polyhydroxyalkanoate, Cellulose Acetate, and Their Engineered Blends by Solvent Casting. *J. Mater. Eng. Perform.* **2020**, *29*, 5542–5556. [CrossRef]
25. Krishnan, S.; Chinnadurai, G.S.; Ravishankar, K.; Raghavachari, D.; Perumal, P. Valorization of agro-wastes for the biosynthesis and characterization of polyhydroxybutyrate by *Bacillus* sp. isolated from rice bran dumping yard. *3 Biotech* **2021**, *11*, 202. [CrossRef] [PubMed]
26. *ASTM D 570-98*; Standard Test Method for Water Absorption of Plastics. ASTM: West Conshohocken, PA, USA, 2018.
27. Behera, S.; Gautam, R.K.; Mohan, S. Polylactic acid and polyhydroxybutyrate coating on hemp fiber: Its effect on hemp fiber reinforced epoxy composites performance. *J. Compos. Mater.* **2022**, *56*, 929–939. [CrossRef]
28. Tejada-Tovar, C.; Villabona-Ortíz, Á.; Ortega-Toro, R. Removal of Metals and Dyes in Water Using Low-Cost Agro-Industrial Waste Materials. *Appl. Sci.* **2023**, *13*, 8481. [CrossRef]
29. Fernández-Pérez, A.; Marbán, G. Visible Light Spectroscopic Analysis of Methylene Blue in Water. *J. Appl. Spectrosc.* **2022**, *88*, 1284–1290. [CrossRef]
30. González-Delgado, A.; Villabona-Ortíz, A.; Tejada-Tovar, C. Evaluation of Three Biomaterials from Coconut Mesocarp for Use in Water Treatments Polluted with an Anionic Dye. *Water* **2022**, *14*, 408. [CrossRef]
31. Pérez-Calderón, J.; Scian, A.; Ducos, M.; Santos, V.; Zaritzky, N. Performance of oxalic acid-chitosan/alumina ceramic biocomposite for the adsorption of a reactive anionic azo dye. *Environ. Sci. Pollut. Res.* **2021**, *28*, 67032–67052. [CrossRef]
32. Kathirselvam, M.; Kumaravel, A.; Arthanarieswaran, V.P.; Saravanakumar, S.S. Characterization of cellulose fibers in Thespesia populnea barks: Influence of alkali treatment. *Carbohydr. Polym.* **2019**, *217*, 178–189. [CrossRef]
33. Shanmugasundaram, N.; Rajendran, I.; Ramkumar, T. Characterization of untreated and alkali treated new cellulosic fiber from an Areca palm leaf stalk as potential reinforcement in polymer composites. *Carbohydr. Polym.* **2018**, *195*, 566–575. [CrossRef] [PubMed]
34. Satha, H.; Kouadri, I.; Benachour, D. Thermal, Structural and Morphological Studies of Cellulose and Cellulose Nanofibers Extracted from Bitter Watermelon of the Cucurbitaceae Family. *J. Polym. Environ.* **2020**, *28*, 1914–1920. [CrossRef]
35. Zhao, X.; Anwar, I.; Zhang, X.; Pellicciotti, A.; Storts, S.; Nagib, D.A.; Vodovotz, Y. Thermal and Barrier Characterizations of Cellulose Esters with Variable Side-Chain Lengths and Their Effect on PHBV and PLA Bioplastic Film Properties. *ACS Omega* **2021**, *6*, 24700–24708. [CrossRef]
36. Vijay, R.; Lenin Singaravelu, D.; Vinod, A.; Sanjay, M.R.; Siengchin, S.; Jawaid, M.; Khan, A.; Parameswaranpillai, J. Characterization of raw and alkali treated new natural cellulosic fibers from Tridax procumbens. *Int. J. Biol. Macromol.* **2019**, *125*, 99–108. [CrossRef]
37. Guerrero, Y. Extracción de la Celulosa a Partir de los Residuos de pasto Común (*Festuca arundinacea*) para la Elaboración de Acetato de Celulosa. Bachelor's Thesis, University Politécnica Salesiana, Sede Cuenca, Cuenca, 2021.
38. Wang, J.; Cahyadi, A.; Wu, B.; Pee, W.; Fane, A.G.; Chew, J.W. The roles of particles in enhancing membrane filtration: A review. *J. Memb. Sci.* **2020**, *595*, 117570. [CrossRef]

39. Aiman Suhaimi, U.; Mohamed, R.M. The properties of coconut coir fiber reinforced epoxy composites. *Int. J. Synerg. Eng. Technol.* **2021**, *2*, 16–35.
40. Battisti, R.; Hafemann, E.; Claumann, C.A.; Machado, R.A.F.; Marangoni, C. Synthesis and characterization of cellulose acetate from royal palm tree agroindustrial waste. *Polym. Eng. Sci.* **2019**, *59*, 891–898. [CrossRef]
41. Cindradewi, A.W.; Bandi, R.; Park, C.W.; Park, J.S.; Lee, E.A.; Kim, J.K.; Kwon, G.J.; Han, S.Y.; Lee, S.H. Preparation and characterization of cellulose acetate film reinforced with cellulose nanofibril. *Polymers* **2021**, *13*, 17. [CrossRef] [PubMed]
42. Zhu, F.; Zheng, Y.M.; Zhang, B.G.; Dai, Y.R. A critical review on the electrospun nanofibrous membranes for the adsorption of heavy metals in water treatment. *J. Hazard. Mater.* **2021**, *401*, 123608. [CrossRef]
43. Unugul, T.; Nigiz, F.U. Preparation and Characterization an Active Carbon Adsorbent from Waste Mandarin Peel and Determination of Adsorption Behavior on Removal of Synthetic Dye Solutions. *Water. Air. Soil Pollut.* **2020**, *231*, 538. [CrossRef]
44. Nandiyanto, A.; Oktiani, R.; Ragadhita, R. How to Read and Interpret FTIR Spectroscope of Organic Material. *Indones. J. Sci. Technol.* **2019**, *4*, 97–118. [CrossRef]
45. Mosoarca, G.; Vancea, C.; Popa, S.; Gheju, M.; Boran, S. Syringa vulgaris leaves powder a novel low-cost adsorbent for methylene blue removal: Isotherms, kinetics, thermodynamic and optimization by Taguchi method. *Sci. Rep.* **2020**, *10*, 17676. [CrossRef] [PubMed]
46. Chen, X.; Liu, L.; Luo, Z.; Shen, J.; Ni, Q.; Yao, J. Facile preparation of a cellulose-based bioadsorbent modified by hPEI in heterogeneous system for high-efficiency removal of multiple types of dyes. *React. Funct. Polym.* **2018**, *125*, 77–83. [CrossRef]
47. Luis-Zarate, V.H.; Rodriguez-Hernandez, M.C.; Alatriste-Mondragon, F.; Chazaro-Ruiz, L.F.; Rangel-Mendez, J.R. Coconut endocarp and mesocarp as both biosorbents of dissolved hydrocarbons in fuel spills and as a power source when exhausted. *J. Environ. Manag.* **2018**, *211*, 103–111. [CrossRef] [PubMed]
48. Bakatula, E.N.; Richard, D.; Neculita, C.M.; Zagury, G.J. Determination of point of zero charge of natural organic materials. *Environ. Sci. Pollut. Res.* **2018**, *25*, 7823–7833. [CrossRef]
49. Shoukat, S.; Bhatti, H.N.; Iqbal, M.; Noreen, S. Mango stone biocomposite preparation and application for crystal violet adsorption: A mechanistic study. *Microporous Mesoporous Mater.* **2017**, *239*, 180–189. [CrossRef]
50. Moosavi, S.M.; Ghassabian, S. Linearity of Calibration Curves for Analytical Methods: A Review of Criteria for Assessment of Method Reliability. In *Calibration and Validation of Analytical Methods—A Sampling of Current Approaches*; IntechOpen: London, UK, 2018.
51. Consiglio Kasemodel, M.; Romão, E.L.; Bueno Ruiz Papa, T. Adsorption of methylene blue on babassu coconut (*Orbignya speciosa*) mesocarp commercial biochar. *Int. J. Environ. Sci. Technol.* **2023**, *21*, 1671–1682. [CrossRef]
52. Pastre, M.M.G.; Cunha, D.L.; Kuznetsov, A.; Archanjo, B.S.; Marques, M. Optimization of Methylene Blue Removal from Aqueous Media by Photocatalysis and Adsorption Processes Using Coconut Biomass-Based Composite Photocatalysts. *Water. Air. Soil Pollut.* **2024**, *235*, 207. [CrossRef]
53. Mishra, L.; Basu, G. Coconut fibre: Its structure, properties and applications. In *Handbook of Natural Fibres*, 2nd ed.; Kozłowski, R.M., Mackiewicz-Talarczyk, M., Eds.; Woodhead Publishing: Sawston, UK, 2020; pp. 231–255.
54. Etim, U.J.; Umoren, S.A.; Eduok, U.M. Coconut coir dust as a low cost adsorbent for the removal of cationic dye from aqueous solution. *J. Saudi Chem. Soc.* **2016**, *20*, S67–S76. [CrossRef]
55. de Oliveira, F.M.; Coelho, L.M.; de Melo, E.I. Avaliação de processo adsortivo utilizando mesocarpo de coco verde para remoção do corante azul de metileno. *Matéria* **2018**, *23*, e12223. [CrossRef]
56. Benhalima, T.; Ferfera-Harrar, H. Eco-friendly porous carboxymethyl cellulose/dextran sulfate composite beads as reusable and efficient adsorbents of cationic dye methylene blue. *Int. J. Biol. Macromol.* **2019**, *132*, 126–141. [CrossRef] [PubMed]
57. Wang, Y.; Zhang, C.; Zhao, L.; Meng, G.; Wu, J.; Liu, Z. Cellulose-based porous adsorbents with high capacity for methylene blue adsorption from aqueous solutions. *Fibers Polym.* **2017**, *18*, 891–899. [CrossRef]
58. Putri, K.N.A.; Keereerak, A.; Chinpa, W. Novel cellulose-based biosorbent from lemongrass leaf combined with cellulose acetate for adsorption of crystal violet. *Int. J. Biol. Macromol.* **2020**, *156*, 762–772. [CrossRef]
59. Rathi, B.S.; Kumar, P.S. Application of adsorption process for effective removal of emerging contaminants from water and wastewater. *Environ. Pollut.* **2021**, *280*, 116995. [CrossRef] [PubMed]
60. Padmavathy, K.S.; Madhu, G.; Haseena, P.V. A study on Effects of pH, Adsorbent Dosage, Time, Initial Concentration and Adsorption Isotherm Study for the Removal of Hexavalent Chromium (Cr (VI)) from Wastewater by Magnetite Nanoparticles. *Procedia Technol.* **2016**, *24*, 585–594. [CrossRef]
61. Sarker, N.; Fakhruddin, A.N.M. Removal of phenol from aqueous solution using rice straw as adsorbent. *Appl. Water Sci.* **2017**, *7*, 1459–1465. [CrossRef]
62. Somsesta, N.; Piyamawadee, C.; Sricharoenchaikul, V.; Aht-Ong, D. Adsorption isotherms and kinetics for the removal of cationic dye by Cellulose-based adsorbent biocomposite films. *Korean J. Chem. Eng.* **2020**, *37*, 1999–2010. [CrossRef]
63. Hariani, P.L.; Riyanti, F.; Kurniaty, A. Modification of cellulose with acetic acid to removal of methylene blue dye. *J. Phys. Conf. Ser.* **2019**, *1282*, 012079. [CrossRef]
64. Salah omer, A.; AEl Naeem, G.; Abd-Elhamid, A.I.; OMFarahat, O.; AEl-Bardan, A.; MASoliman, H.; Nayl, A.A. Adsorption of Crystal violet and Methylene blue Dyes using a Cellulose-based adsorbent from Sugercane bagasse: Characterization, kinetic and Isotherm studies. *J. Mater. Res. Technol.* **2022**, *19*, 3241–3254. [CrossRef]

65. Alibak, A.H.; Khodarahmi, M.; Fayyazsanavi, P.; Alizadeh, S.M.; Hadi, A.J.; Aminzadehsarikhanbeglou, E. Simulation the adsorption capacity of polyvinyl alcohol/carboxymethyl cellulose based hydrogels towards methylene blue in aqueous solutions using cascade correlation neural network (CCNN) technique. *J. Clean. Prod.* **2022**, *337*, 130509. [CrossRef]
66. Araújo, R.F.; Bezerra, L.C.A.; de Novais, L.M.R.; D'Oca, C.D.R.M.; Avelino, F. Unveiling the mechanistic aspects of methylene blue adsorption onto a novel phosphate-decorated coconut fiber lignin. *Int. J. Biol. Macromol.* **2023**, *253*, 127011. [CrossRef] [PubMed]
67. Goscianska, J.; Ciesielczyk, F. Lanthanum enriched aminosilane-grafted mesoporous carbon material for efficient adsorption of tartrazine azo dye. *Microporous Mesoporous Mater.* **2019**, *280*, 7–19. [CrossRef]
68. Bhowmik, S.; Chakraborty, V.; Das, P. Batch adsorption of indigo carmine on activated carbon prepared from sawdust: A comparative study and optimization of operating conditions using Response Surface Methodology. *Results Surf. Interfaces* **2021**, *3*, 100011. [CrossRef]
69. Castro, D.; Rosas-Laverde, N.M.; Belén Aldás, M.; Almeida-Naranjo, C.E.; Guerrero, V.H.; Iuliana Pruna, A.; Aldás, N.M.; Almeida-Naranjo, M.B.; Guerrero, C.E.; Pruna, V.H.; et al. Chemical Modification of Agro-Industrial Waste-Based Bioadsorbents for Enhanced Removal of Zn(II) Ions from Aqueous Solutions. *Materials* **2021**, *14*, 2134. [CrossRef] [PubMed]
70. Jawad, A.H.; Abdulhameed, A.S.; Mastuli, M.S. Acid-factionalized biomass material for methylene blue dye removal: A comprehensive adsorption and mechanism study. *J. Taibah Univ. Sci.* **2020**, *14*, 305–313. [CrossRef]
71. Jasper, E.E.; Ajibola, V.O.; Onwuka, J.C. Nonlinear regression analysis of the sorption of crystal violet and methylene blue from aqueous solutions onto an agro-waste derived activated carbon. *Appl. Water Sci.* **2020**, *10*, 132. [CrossRef]

Disclaimer/Publisher's Note: The statements, opinions and data contained in all publications are solely those of the individual author(s) and contributor(s) and not of MDPI and/or the editor(s). MDPI and/or the editor(s) disclaim responsibility for any injury to people or property resulting from any ideas, methods, instructions or products referred to in the content.